Syntheses and Conformations of Somatostatin-Related Cyclic Hexapeptides Incorporating Specific α- and β-Methylated Residues

Ya-Bo He,† Ziwei Huang,† Karen Raynor,‡ Terry Reisine,‡ and Murray Goodman*,†

Contribution from the Department of Chemistry, 0343, University of California, San Diego, La Jolla, California 92093, and the Department of Pharmacology, University of Pennsylvania, Philadelphia, Pennsylvania 19104

Received February 19, 1993

Abstract: The cyclic hexapeptide c[-Pro⁶-Phe⁷-D-Trp⁸-Lys⁹-Thr¹⁰-Phe¹¹-] displays high biological activities in inhibiting the release of many bioactive molecules, including growth hormone, insulin, and glucagon. The superscript numbers refer to the location of the residues in native somatostatin. Conformational studies of this cyclic hexapeptide indicated considerable conformational flexibility in various regions of backbone and side chains. The flexibility prevents the elucidation of the "bioactive conformation" of this molecule when bound to a receptor. To reduce the conformational flexibility, we have synthesized one main chain methylated analog containing α-MeVal at position 10, c[-Pro⁶-Phe⁷-D-Trp⁸-Lys⁹-(*S*)-α-MeVal¹⁰-Phe¹¹-], and two side chain methylated analogs containing β-MeTrp and β-MePhe at positions 8 and 11, respectively, c[-Pro⁶-Phe⁷-(*2R,3S*)-β-MeTrp⁸-Lys⁹-Thr¹⁰-(*2S,3S*)-β-MePhe¹¹-] and c[-Pro⁶-Phe⁷-(*2S,3R*)-β-MeTrp⁸-Lys⁹-Thr¹⁰-(*2S,3S*)-β-MePhe¹¹-]. The effect of main chain and side chain methylations has been studied using 500-MHz two-dimensional ^{1}H-NMR and computer simulations. These main chain and side chain methylated analogs display constrained conformational preferences at the modified backbone and side chains. One of the side chain methylated analogs shows high potency in receptor binding. Conformational studies of these analogs provide valuable information about the main chain and side chain conformation required for receptor interaction. This study clearly demonstrated a novel approach using main chain and side chain methylations in the elucidation of the bioactive conformation of somatostatin analogs. This approach may have important implications in the study of other peptide hormones and neurotransmitters.

Introduction

Somatostatin is a cyclic tetradecapeptide hormone, Ala¹-Gly²-c[-Cys³-Lys-⁴-Asn⁵-Phe⁶-Phe⁷-Trp⁸-Lys⁹-Thr¹⁰-Phe¹¹-Thr¹²-Ser¹³-Cys¹⁴-], which was isolated from ovine hypothalami in 1973.[1] First known for its ability to inhibit the release of growth hormone,[1] somatostatin also suppresses the release of many other bioactive molecules, including glucagon, insulin, gastrin, and secretin.[2-4]

Because somatostatin has a wide range of physiological roles and clinical applications, extensive studies have been carried out to investigate its structure–activity relationships. Particular focus has been on the design of cyclic constrained analogs related to somatostatin with a smaller backbone ring size. This led to the synthesis of a highly potent analog of somatostatin by Veber and co-workers, c[-Pro⁶-Phe⁷-D-Trp⁸-Lys⁹-Thr¹⁰-Phe¹¹-] (**I**), which employs a Phe¹¹-Pro⁶ bridge to cyclize the residues 7–10 in native somatostatin.[5] The superscript numbers following amino acid designations indicate the location of the residues in native somatostatin. From NMR studies, Veber proposed a β II′ turn around D-Trp⁸-Lys⁹ and a β VI turn around Phe¹¹-Pro⁶ with a *cis* amide bond.[6]

Since its discovery, the cyclic hexapeptide **I** has been the subject of extensive structure–activity studies.[7-10] We have carried out conformational analyses using NMR experiments and computer simulations for the cyclic hexapeptide **I**. Our studies indicated that this molecule (**I**) displays considerable conformational flexibility around the backbones of Phe⁷ and Thr¹⁰ and the side chains of Phe⁷, Trp⁸, and Phe¹¹.[11] To reduce the conformational flexibility of this peptide (**I**), we recently synthesized a series of cyclic hexapeptide analogs of somatostatin containing α- and β-methyl substitutions.[12] Studies of bioactive peptides containing α- and β-methylated residues were previously carried out in other laboratories. Marshall and co-workers synthesized bradykinin[13] and angiotensin II[14] analogs containing α-methylated residues and suggested that the α-methyl substitution resulted in a dramatic reduction of the conformational space available to the backbone of the modified residue. Hruby and co-workers synthesized cyclic enkephalin analogs utilizing β-MePhe and suggested that the side chain of the β-methylated residue was constrained to prefer

* To whom correspondence should be addressed.
† University of California, San Diego.
‡ University of Pennsylvania.

(1) Brazcau, P.; Vale, W.; Burgus, R.; Ling, N.; Bucher, M.; Rivier, J.; Guillemin, R. *Science* **1973**, *179*, 77–79.
(2) Koerker, D. J.; Harker, L. A.; Goodner, C. J. *N. Engl. J. Med.* **1975**, *293*, 476–479.
(3) Gerich, J. E.; Lovinger, R.; Grodsky, G. M. *Endocrinology* **1975**, *96*, 749–754.
(4) Johansson, C.; Wiscn, O.; Efendic, S.; Uvnas-Wallensten, K. *Digestion* **1981**, *22*, 126–137.
(5) Veber, D. F.; Freidinger, R. M.; Perlow, D. S.; Palaveda, W. J., Jr.; Holly, F. W.; Strachan, R. G.; Nutt, R. F.; Arison, B. J.; Homnick, C.; Randall, W. C.; Glitzer, M. S.; Saperstein, R.; Hirschmann, R. *Nature* **1981**, *292*, 55–58.
(6) Veber, D. F. In *Peptides, Synthesis, Structure and Function, Proceedings of the Seventh American Peptide Symposium*; Rich, D. H., Gross, V. J., Eds.; Pierce Chemical Co.: Rockford, IL, 1981, pp 685–694.
(7) Nutt, R. F.; Saperstein, R.; Veber, D. F. In *Peptides, Structure and Function, Proceedings of the Eighth American Peptide Symposium*; Hruby, V. J., Rich, D. H., Eds.; Pierce Chemical Co.: Rockford, IL, 1983, pp 345–348.
(8) Nutt, R. F.; Curley, P. E.; Pitzenberger, S. M.; Freidinger, R. M.; Saperstein, R.; Veber, D. F. In *Peptides, Structure and Function, Proceedings of the Ninth American Peptide Symposium*; Deber, C. M., Hruby, V., Kopple, K. D., Eds.; Peirce Chemical Co.: Rockford, IL, 1985; pp 441–444.
(9) Nutt, R. F.; Colton, C. D.; Saperstein, R.; Veber, D. F. In *Somatostatin*; Reichlin, S., Ed.; Plenum Publishing Corp.: New York, 1987; pp 83–88.
(10) Veber, D. F. In *Peptides: Chemistry and Biology, Proceedings of the Twelfth American Peptide Symposium*; Smith, J. A., Rivier, J. E., Eds.; ESCOM: Leiden, 1992; pp 3–14.
(11) Huang, Z. Ph.D. Thesis, University of California, 1993.
(12) Huang, Z.; He, Y.-B.; Raynor, K.; Tallent, M.; Reisine, T.; Goodman, M. *J. Am. Chem. Soc.* **1992**, *114*, 9390–9401.
(13) Turk, J.; Needleman, P.; Marshall, G. R. *J. Med. Chem.* **1975**, *18*, 1139–1142.
(14) Turk, J.; Needleman, P.; Marshall, G. R. *Mol. Pharmacol.* **1976**, *12*, 217–224.

0002-7863/93/1515-8066$04.00/0

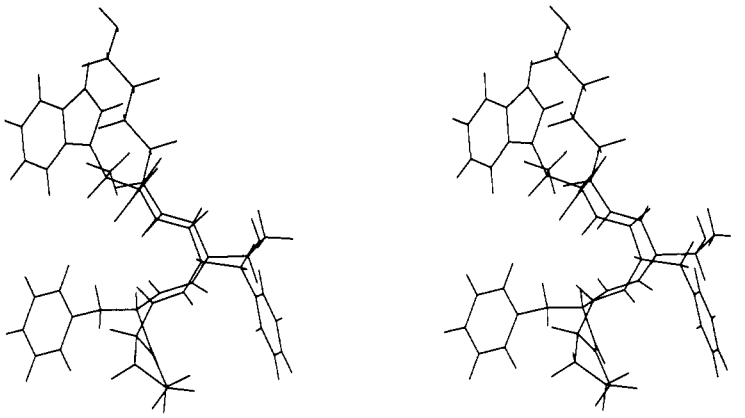

Figure 1. Stereoview of the folded conformations of c[-Pro^6-Phe^7-(*2R,3S*)-β-MeTrp^8-Lys^9-Thr^{10}-Phe^{11}-]. We suggested that the folded conformation is the bioactive conformation for somatostatin analogs.[12]

a particular side chain rotamer.[15] In our study of the somatostatin analog containing α-MePhe^7, we found that this α-methylated analog displayed a constrained "flat" conformation because of the α-methylation at position 7, which led to the loss of its binding affinity to the somatostatin receptor. As for the somatostatin analogs containing β-methylated residues, we found that the β-methylations had dramatic effects on constraining the side chain conformation of the modified residue. This resulted in significant changes in the binding potency of these β-methylated analogs. Analyses of the different conformational and biological profiles observed for these β-methylated analogs in NMR experiments and computer simulations allowed us to derive the possible "bioactive conformations" for the side chains of Phe^7, D-Trp^8, and Phe^{11}. Combining our findings from the α- and β-methylated analogs, we were able to suggest a "folded" conformation for somatostatin analogs when bound to a receptor (Figure 1). In this model, the Trp^8 side chain assumes the *trans* rotamer while the Lys^9 side chain assumes the *gauche*– (*g*$^-$) rotamer, thus allowing a close proximity between these two side chains. The Phe^{11} side chain assumes the *trans* rotamer. The peptide backbone adopts a β II′ turn about Trp^8-Lys^9 and a β VI turn about Phe^{11}-Pro^6. The overall structure is folded about the Phe^7 and Thr^{10} residues, assuming a C_7 conformation for their φ and Ψ torsions.

In this paper, we report the studies of additional somatostatin analogs containing α- and di-β-methylated residues in an attempt to examine our proposed folded model. According to the model, the peptide backbone is folded about Phe^7 and Thr^{10}. Previous studies of the α-MePhe^7 analog suggested that this molecule adopts a flat conformation because of the α-methylation at position 7, which led to the loss of binding activity.[12] This allowed us to propose that the flat conformation is not the bioactive conformation. To examine our proposal further, we have synthesized the cyclic hexapeptide c[-Pro^6-Phe^7-D-Trp^8-Lys^9-(*S*)-α-MeVal^{10}-Phe^{11}-] (**II**), which contains α-methylvaline (α-MeVal) at position 10. This new α-methylated analog is also expected to adopt a flat conformation similar to that for the α-MePhe^7 analog because of the α-methylation at position 10. From these studies, we will be able to relate another somatostatin analog with a flat conformation to bioactivity. We employed the α-MeVal^{10} residue since this substitution for Thr^{10} has been shown to yield highly active analogs.[10]

To investigate the side chain conformations of somatostatin analogs, we have synthesized analogs containing β-methylations at both position 8 and 11. The β-methylation at position 7 is not used here because previous findings showed that the β-methylation at position 7 has no effect on the binding potency.[12] As for the β-methylation at positions 8 and 11, our previous studies showed that the chiralities of *2R,3S* or *2S,3R* for the β-MeTrp^8 residue and *2S,3S* for the β-MePhe^{11} residue are required for bioactivity.[12]

(15) Hruby, V. J.; Toth, G.; Gehrig, C. A.; Kao, L.-F.; Knapp, R.; Lui, G. K.; Yamamura, H. I.; Kramer, T. H.; Davis, P.; Burks, T. F. *J. Med. Chem.* **1991**, *34*, 1823.

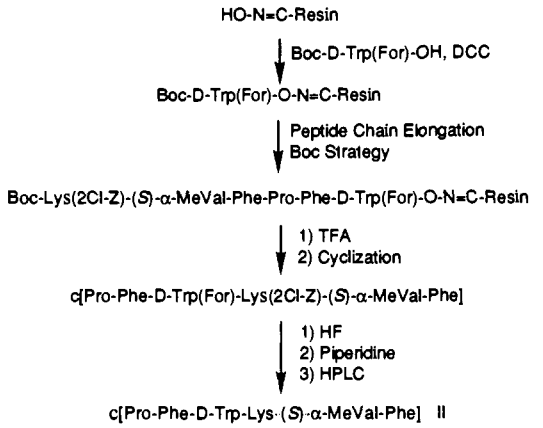

Figure 2. Scheme for the synthesis of analog **II**.

Therefore, we synthesized two cyclic hexapeptides, c[-Pro^6-Phe^7-(*2R,3S*)-β-MeTrp^8-Lys^9-Thr^{10}-(*2S,3S*)-β-MePhe^{11}-] (**III**) and c[-Pro^6-Phe^7-(*2S,3R*)-β-MeTrp^8-Lys^9-Thr^{10}-(*2S,3S*)-β-MePhe^{11}-] (**IV**), containing β-methylations at both position 8 and 11. We anticipated that these di-β-methylated analogs will display the combined effect from the mono-β-methylation at positions 8 and 11, which should provide important information about the bioactive conformation for the side chains at positions 8 and 11.

Synthesis

Syntheses of racemic α-methylvaline (α-MeVal) were carried out according to literature procedure.[16] Optically pure (*S*)-α-MeVal was obtained by enzymatic hydrolysis[17] and was converted to methyl ester, followed by coupling with Boc-Lys(2Cl-Z)-OH[18] to form Boc-Lys(2Cl-Z)-(*S*)-α-MeVal-OMe. Hydrolysis of the methyl ester provided Boc-Lys(2Cl-Z)-(*S*)-α-MeVal-OH. This approach was employed because of the poor yield obtaned when an amino protecting group, such as Boc, was initially applied. The above dipeptide was used for segment condensation in the peptide synthesis. The cyclic hexapeptide c[-Pro-Phe-D-Trp-Lys-(*S*)-α-MeVal-Phe-] (**II**) was synthesized on a *p*-nitrobenzophenone oxime resin[12] (Figure 2). The synthesis was carried out by starting from Boc-D-Trp(For)-OH linked to a resin. The peptide chain was then assembled by consecutive cleavage steps of Boc groups and addition of the *N*-Boc-amino acids. After removal of the last Boc group from the N-terminal residue, the liberated

(16) Kurona, K. *Biochem. Z.* **1922**, *134*, 434.

(17) Turk, J.; Panse, G. T.; Marshall, G. R. *J. Org. Chem.* **1975**, *40*, 953–955.

(18) Abbreviations used are those recommended by the IUPAC-IUB Commission: Bzl, benzyl; 2Cl-Z, ((2-chlorobenzyl)oxy)carbonyl; Boc, (*tert*-butyloxy)carbonyl; For, formyl; Fmoc, ((9-fluorenylmethyl)oxy)carbonyl; DCC, dicyclohexylcarbodiimide; BOP, (benzotriazol-1-yloxy)tris(dimethylamino)phosphonium hexafluorophosphate; DPPA, diphenylphosphoryl azide; TFA, trifluoroacetic acid; DIEA, diisopropylethylamine; DCM, dichloromethane.

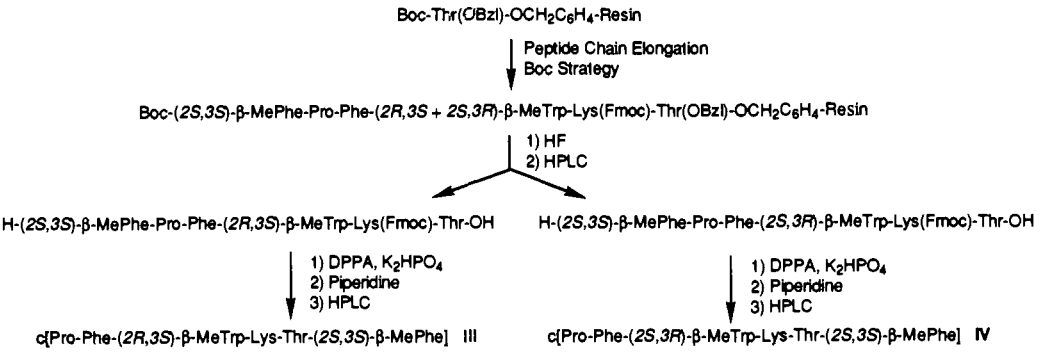

Figure 3. Scheme for the syntheses of analogs **III** and **IV**.

Table I. Binding Constants for Somatostatin Analogs

	analog	IC_{50} (nM)
I	c[-Pro-Phe-D-Trp-Lys-Thr-Phe-]	1
II	c[-Pro-Phe-D-Trp-Lys-(*S*)-α-MeVal-Phe-]	1000
III	c[-Pro-Phe-(*2R,3S*)-β-MeTrp-Lys-Thr-(*2S,3S*)-β-MePhe-]	7
IV	c[-Pro-Phe-(*2S,3R*)-β-MeTrp-Lys-Thr-(*2S,3S*)-β-MePhe-]	1000
V	c[-Pro-Phe-(*2R,3S*)-β-MeTrp-Lys-Thr-Phe-]	<1[a]
VI	c[-Pro-Phe-(*2S,3R*)-β-MeTrp-Lys-Thr-Phe-]	10[a]
VII	c[-Pro-Phe-D-Trp-Lys-Thr-(*2S,3S*)-β-MePhe-]	50[a]

[a] See ref 12.

amino group was allowed to react with the activated C-terminus attached to the resin, thereby releasing the side chain protected cyclic hexapeptide derivative. The protecting groups 2Cl-Z and For were removed by HF and piperidine treatment, respectively. The final cyclic hexapeptide **II** was purified by preparative RP-HPLC.

The amino acid derivatives β-methylphenylalanine (β-MePhe), Boc-(*2S,3S*)-β-MePhe-OH, and the threo isomers of β-methyltryptophan [(*2R,3S* + *2S,3R*)-β-MeTrp] and Boc-(*2R,3S* + *2S,3R*)-β-MeTrp-OH were prepared according to our recent report.[12] Cyclic hexapeptides c[-Pro-Phe-(*2R,3S*)-β-MeTrp-Lys-Thr-(*2S,3S*)-β-MePhe-] (**III**) and c[-Pro-Phe-(*2S,3R*)-β-MeTrp-Lys-Thr-(*2S,3S*)-β-MePhe-] (**IV**) were synthesized on Merrifield resin followed by cyclization in solution using the same method as the previous report[12] (Figure 3). After the linear hexapeptide chain was assembled, the peptide was cleaved by HF from the resin, and the resulting two diastereomers of the linear hexapeptides were separated by RP-HPLC. The cyclization of each compound was performed in DMF using DPPA as a coupling reagent. After removal of the Fmoc group on Lys, the final product was purified by RP-HPLC. The absolute configuration of the C^{α} atom on the β-MeTrp residue in each final product was determined by NMR.[19] The absolute configuration of the C^{β} atom could then be simply deduced, since the relative configuration between C^{α} and C^{β} atoms was previously established.

Results

The α-methylated and di-β-methylated analogs were measured for specific binding to the somatostatin receptor. Their potencies are presented in Table I. We also include the binding potencies for c[-Pro-Phe-D-Trp-Lys-Thr-Phe-] (**I**) synthesized by Veber and co-workers[5] (compound **I** will be referred to as the parent compound hereafter) and some mono-β-methylated analogs we prepared before.

The NMR data, including NOEs, $J_{NH-H\alpha}$ and $J_{H\alpha\beta}$ vicinal coupling constants, temperature coefficients of amide protons, and changes in chemical shifts, were used to analyze main chain and side chain conformational preferences. The NOEs provide the most important information about backbone conformations by indicating relative proton–proton distances (Table II). Further information about backbone conformations was derived from vicinal coupling constants $J_{NH-H\alpha}$, from which the torsion ϕ was calculated using a Karplus-type equation.[20,21] The vicinal coupling constants $J_{NH-H\alpha}$ are given in Table III for all analogs. Temperature coefficients for the amide protons also provide information on backbone conformations by indicating solvent shielding or intramolecular hydrogen bonding. As shown in Table IV, the Thr^{10} or α-MeVal NH proton displays small temperature coefficients for all analogs, which indicates its involvement in intramolecular hydrogen bonding.

As for the side chain conformations, vicinal coupling constants $J_{H\alpha\beta}$ offer the most important information on side chain torsions

Table II. Summary of the Backbone Interresidue NOEs Observed for the α-Methylated Analog **II** and β-Methylated Analogs **III** and **IV**[a]

	II	III	IV
NOE(Pro^6 $C^{\alpha}H$–Phe^7 NH)	w	w	–
NOE(Pro^6 $C^{\delta}H$–Phe^7 NH)	–	–	–
NOE(Phe^7 $C^{\alpha}H$–Trp^8 NH)	s	s	s
NOE(Trp^8 $C^{\alpha}H$–Lys^9 NH)	s	s	s
NOE(Lys^9 NH–Thr^{10} NH)	na	m	m
NOE(Lys^9 NH–α-$MeVal^{10}$ NH)	m	na	na
NOE(Thr^{10} $C^{\alpha}H$–Phe^{11} NH)	na	s	s
NOE(α-$MeVal^{10}$ α-Me–Phe^{11} NH)	s	na	na
NOE(Phe^{11} $C^{\alpha}H$–Pro^6 $C^{\alpha}H$)	s	s	s
NOE(Phe^{11} $C^{\alpha}H$–Pro^6 $C^{\delta}H$)	–	–	–

[a] The observed NOEs are qualitatively classified according to their intensities: s, strong; m, medium; w, weak; –, absent; na, not applicable.

Table III. Vicinal Coupling Constants[a] $J_{NH-H\alpha}$ Observed for Analogs **I–IV**

	analogs			
residue	I	II	III	IV
Phe^7	*b*	5.58	6.28	9.45
D-Trp^8	7.81	9.02	7.95	5.59
Lys^9	6.99	7.52	7.52	7.09
Xxx^{10} [d]	7.36	*c*	7.51	7.52
Phe^{11}	4.95	6.01	5.80	1.93

[a] Values in hertz. [b] Due to excessive overlap, the coupling constant could not be measured. [c] The vicinal coupling constant $J_{NH-H\alpha}$ is not applicable to the α-MeVal residue. The Xxx residue is α-MeVal in compound **II** and Thr in the others.

Table IV. Temperature Coefficients[a] of Amide Proton Chemical Shifts of Analogs **I–IV**

	analogs			
residue	I	II	III	IV
Phe^7	1.6	–0.9	3.0	4.3
D-Trp^8	5.1	5.2	5.9	2.1
Lys^9	5.4	6.8	5.4	4.3
Xxx^{10} [b]	0.3	0.8	–0.2	–1.7
Phe^{11}	2.8	5.8	2.5	7.6

[a] Values in –ppb/K. [b] The Xxx residue is α-MeVal in compound **II** and Thr in the others.

(19) Yamazaki, T.; Goodman, M. *Chirality* **1991**, *3*, 1–9.

(20) Bystrov, V. F.; Ivanov, V. T.; Portnova, S. L.; Balashova, T. A.; Ovchinnikov, Y. A. *Tetrahedron* **1973**, *29*, 873–877.

Table V. $^3J_{H\alpha\beta}$ Coupling Constants[a] and Calculated Side Chain Populations for χ_1[b] for Di-β-methylated Somatostatin Analogs **III, IV**

	analogs		
residue	parent (**I**)	**III**	**IV**
Phe[7]	5.92, 5.90	6.98, 5.69	3.98, 12.14
$f(g^-)$	0.23	0.21	0.83
$f(t)$	0.23	0.33	0.04
$f(g^+)$	0.54	0.46	0.13
Trp[8]	8.10, 7.22	10.52[c]	7.73[c]
$f(g^-)$	0.20		
$f(t)$	0.44	0.68	0.40
$f(g^+)$	0.36		
Lys[9]	4.00, 10.09	3.43, 10.09	15.04[d]
$f(g^-)$	0.68	0.68	
$f(t)$	0.13	0.08	
$f(g^+)$	0.19	0.24	0.10
Thr[10] [e]	4.42	4.08	6.45
$f(g^-)$	0.17	0.14	0.35
Phe[11]	7.15, 8.40	8.37[c]	5.68[c]
$f(g^-)$	0.35	0.47	0.21
$f(t)$	0.47		
$f(g^+)$	0.18		

[a] Values are in hertz. [b] $f(g^-)$, $f(t)$, and $f(g^+)$ represent the fraction of the χ_1 population in the *gauche*−, *trans*, and *gauche*+ rotamers, respectively. [c] Because β-methylated residues have a single β-proton, only one rotamer can be estimated, depending on the chiralities of the C^α and C^β atoms. [d] The reported value is for $J_{H\alpha\beta1} + J_{H\alpha\beta2}$. $J_{H\alpha\beta1}$ and $J_{H\alpha\beta2}$ were difficult to measure because of overlap. Analyzing the multiplicity of the α proton resonance and utilizing the $J_{NH-H\alpha}$ coupling constant give $J_{H\alpha\beta1} + J_{H\alpha\beta2}$. From this value, the population $f(g^+)$ for an L residue or $f(g^-)$ for a D residue may be calculated. [e] Because Thr has a single β-proton, only the $f(g^-)$ population can be calculated while the $f(t)$ and $f(g^+)$ populations of χ_1 cannot be distinguished.

χ_1. Using a three-state model, where the energy minima associated with χ_1 are *trans*, g^-, and g^+, the populations in each of these states were calculated using Pachler's equations[22] for nonaromatic amino acid residues and Cung's equations[23] for aromatic residues, respectively (Table V). The observed signals to their respective β-protons were assigned following a procedure described by Yamazaki and co-workers.[24] Changes in chemical shifts may provide additional indications about the relative locations of aromatic side chains. For instance, the upfield shift of Lys[9] C^γ protons may be explained by the shielding by the Trp[8] side chain which is in close proximity with the Lys[9] side chain.[6] By comparing changes in chemical shifts between diastereomers of the β-methylated analogs and the parent compound (**I**), we were able to obtain information about the preferred side chain rotamers for the modified residues. Table VI lists the chemical shifts observed for the representative di-β-methylated analogs.

Discussion

Analog II Containing α-Methylation at Position 10. The NOEs of Trp[8] $C^\alpha H$–Lys[9] NH and Lys[9] NH–Thr[10] NH and the coupling constants of Trp[8] and Lys[9] suggest a β II′ turn about the D-Trp[8]-Lys[9] region. The low temperature coefficient measured for the amide of α-MeVal[10] is consistent with a hydrogen bond between α-MeVal[10] NH and Phe[7] CO, which stabilizes the β II′ turn. As for the bridging region, the strong NOE between Phe[11] $C^\alpha H$ and Pro[6] $C^\alpha H$ indicates a *cis* amide bond. These results suggest that this analog (**II**) maintains similar conformations about the D-Trp[8]-Lys[9] region and the bridging region of the parent compound (**I**). The mutual strong NOEs of Phe[11] NH, the α-methyl group, and $C^\beta H$ of α-MeVal[10] confirm the C_5 conformation for the backbone of the α-MeVal[10] residue because only in the C_5 conformation can the observed NOEs be detected. In the C_7 conformation only the strong NOE of Phe[11] NH and the α-methyl group would be expected. As a result, the α-MeVal[10] analog (**II**) displays a flat conformation (Figure 4). The dihedral angles for this flat conformation are given in Table VII, together with the dihedral angles for our proposed folded model as reference.

Table VI. Chemical Shifts for Analogs **I, III,** and **IV**

		resonance (δ, ppm)		
residue		parent (**I**)	**III**	**IV**
Pro[6]	α	3.72	4.20	2.95
	β	1.07/1.70	1.92/1.55	0.93/1.56
	γ	1.26/1.49	1.40/1.68	0.45/1.34
	δ	3.05/3.21	3.20/3.36	2.95/3.16
Phe[7]	NH	7.20	7.22	8.61
	α	4.56	4.81	4.59
	β	2.76/2.89	2.93/2.99	2.95/3.40
β-MeTrp[8]	NH	8.40	8.66	7.83
	α	4.56	4.36	4.28
	β	2.70/2.95	3.26	3.53
	β-Me		1.01	1.41
Lys[9]	NH	8.67	8.21	7.98
	α	3.81	3.43	3.70
	β	1.43/1.60	1.13/1.40	1.52/1.60
	γ	1.01	0.30	1.02
	δ	1.26	1.13	1.34
	ε	2.49	2.39/2.59	2.59
Thr[10]	NH	6.96	6.95	6.98
	α	4.17	4.05	4.26
	β	3.94	3.79	3.77
	γ	0.99	0.95	1.12
	OH		5.30	
β-MePhe[11]	NH	8.30	7.94	8.52
	α	4.28	4.41	4.22
	β	2.88/2.88	3.05	3.19
	β-Me		1.18	1.27

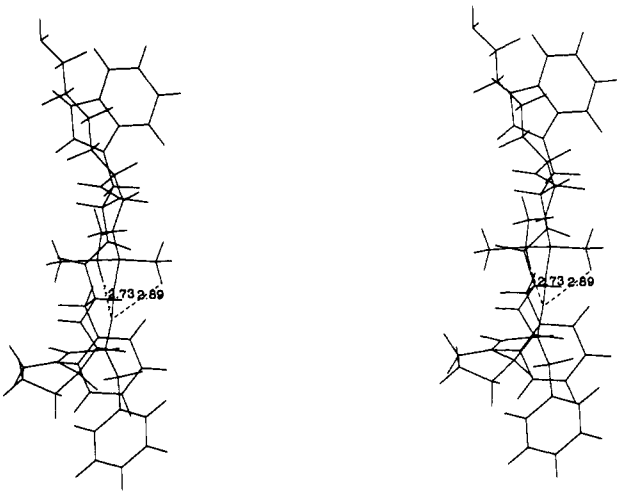

Figure 4. Stereoview of the flat conformation of c[-Pro[6]-Phe[7]-D-Trp[8]-Lys[9]-(*S*)-α-MeVal[10]-Phe[11]-] (**II**). The distances between the Phe[11] NH and the α-methyl group and $C^\beta H$ of α-MeVal[10] are given in angstroms.

Energy minimization studies also indicated that because of the steric effect introduced by the α-methyl group, the backbone of the α-MeVal[10] residue is constrained to prefer the C_5 conformation, and therefore the flat conformation is favored. The α-MeVal[10] analog (**II**) has been tested and displays low binding affinities compared with the parent compound (**I**). As reported in our previous paper, the parent cyclic hexapeptide can adopt two types of conformations: folded and flat, depending on the backbone conformation of Phe[7] and Thr[10] residues. Since the α-MeVal[10] analog adopts only the flat conformation and is inactive in receptor binding, we suggested that the flat conformation is not the bioactive conformation, and the folded conformation is likely the bioactive conformation.

Analogs III and IV Containing β-Methylations at Positions 8 and 11. For analog **III**, NOEs observed for Phe[7] $C^\alpha H$–β-MeTrp[8] NH, β-MeTrp[8] $C^\alpha H$–Lys[9] NH, and Lys[9] NH–Thr[10] NH, together with the measured $J_{NH-H\alpha}$ coupling constants of β-MeTrp[8] and

(21) Cung, M. T.; Marraud, M.; Neel, J. *Macromolecules* **1974**, *7*, 606–613.
(22) Pachler, K. G. P. *Spectrochim. Acta* **1964**, *20*, 581–587.
(23) Cung, M. T.; Marraud, M. *Biopolymers* **1982**, *21*, 953–967.
(24) Yamazaki, T.; Probstl, A.; Schiller, P. W.; Goodman, M. *Int. J. Pept. Protein Res.* **1991**, *37*, 364–381.

Table VII. Dihedral Angles (deg) for the Folded Conformation of c[-Pro^6-Phe^7-(*2R,3S*)-β-MeTrp^8-Lys^9-Thr^{10}-Phe^{11}-] (Figure 1) and the Flat Conformation of c[-Pro^6-Phe^7-D-Trp^8-Lys^9-α-MeVal^{10}-Phe^{11}-] (Figure 4)

		folded conformer in Figure 1	flat conformer in Figure 4
Pro^6	φ	−74	−74
	ψ	−20	−37
Phe^7	φ	−74	−142
	ψ	83	168
	χ1	−54	−59
	χ2	97	100
Trp^8	φ	69	87
	ψ	−139	−139
	χ1	178	176
	χ2	−86	−88
Lys^9	φ	−62	−66
	ψ	−35	−18
	χ1	−62	−62
	χ2	−179	180
Xxx^{10}	φ	−84	−159
	ψ	75	−172
	χ1	58	178
Phe^{11}	φ	−49	−66
	ψ	139	144
	χ1	−174	−177
	χ2	91	91

Lys^9, suggest a β II′ turn around the β-MeTrp^8-Lys^9 region. The low temperature coefficient measured for the Thr^{10} NH proton in these analogs is consistent with a hydrogen bond between Thr^{10} NH and Phe^7 CO, which stabilizes the β II′ turn. For analog **IV**, a β I turn is expected because of the L chirality of the residues at positions i + 1 and i + 2.[25,26] The β I turn is supported by the NOEs observed for Phe^7 C^{β}H–β-MeTrp^8 NH and β-MeTrp^8 C^{β}H–Lys^9 NH. The $J_{NH-H\alpha}$ coupling constants of β-MeTrp^8 and Lys^9 are also in agreement with the β I turn around β-MeTrp^8–Lys^9. Both analogs (**III**, **IV**) display a β VI turn with a *cis* amide bond at the bridging region, which is indicated by the strong NOE between the C^α protons of β-MePhe^{11} and Pro^6.

The β-methylation shows dramatic effects on the conformational preferences of the modified side chains in both di-β-methylated analogs (**III**, **IV**). For analog **III**, the side chains of (*2R,3S*)-β-MeTrp^8 and (*2S,3S*)-β-MePhe^{11} are highly constrained to prefer the *trans* and *g*$^-$ rotamers, respectively. As shown in Table V, the side chain of (*2R,3S*)-β-MeTrp^8 displays a 54% increase in the *trans* rotamer population while the side chain of (*2S,3S*)-β-MePhe^{11} displays a 34% increase in the *g*$^-$ rotamer population when compared with the parent compound (**I**). The changes of chemical shifts between analog **III** and the parent compound (**I**) also provided additional evidence about the constrained side chain rotameric conformations of β-MeTrp^8 and β-MePhe^{11} residues. As shown in Table VI, it is most noteworthy that the C^γ protons in the Lys^9 side chain are shifted significantly upfield to 0.30 ppm in analog **III**. This may be explained by the shielding effect of the indole ring in close proximity with the Lys^9 side chain because the β-MeTrp^8 side chain greatly prefers the *trans* rotameric conformation. Noticeable changes of chemical shifts were also observed for protons in residues 7 and 9, in which the chemical shifts of these protons displayed different trends for analog **III** and the parent compound (**I**). The difference in the chemical shifts of protons in Phe^7 and Lys^9 adjacent to the modified β-MeTrp^8 may be explained by the shielding and deshielding effects from the β-MeTrp^8 side chain in the *trans* rotamer as described above. Similar evidence was obtained for the *g*$^-$ rotamer of β-MePhe^{11} side chain by examining the changes of the chemical shifts of protons in the adjacent Thr^{10} and Pro^6 residues.

As for analog **IV**, the side chain rotameric conformations may not be directly compared with the parent compound (**I**) since different backbone structures were observed around residues 8 and 9. However, a comparison was made between analog **IV** and a cyclic hexapeptide, c[-Pro^6-Phe^7-L-Trp^8-Lys^9-Thr^{10}-Phe^{11}-] (L-Trp^8 analog), which shows similar backbone conformations.[27] The (*2S,3R*)-β-MeTrp^8 side chain in analog **IV** displayed a preference for the *trans* rotamer, as indicated by the upfield shifting of Lys^9 C^γ protons when compared with the L-Trp^8 analog. Meanwhile, the (*2S,3S*)-β-MePhe^{11} side chain in analog **IV** showed a fraction of 21% in the *g*$^-$ rotamer as compared with the essentially 0 population in the L-Trp^8 analog. These results, together with those obtained for analog **III**, are fully consistent with our previous findings from mono-β-methylated analogs that the side chain of the β-methylated residue is constrained to prefer the *g*$^-$ rotamer for the *2S,3S* isomer and the *trans* rotamer for the *2S,3R* and *2R,3S* isomers.[12] It should be pointed out that, although β-methylations do not necessarily result in a predominant population in the constrained rotamer as in cases of the side chain of β-MeTrp^8 in analog **IV** and the side chain of β-MePhe^{11} in analogs **III** and **IV** (Table V), the enhanced preference for a particular side chain rotamer arising from β-methylations is clearly indicated by the increase of rotameric population and changes of chemical shifts as compared with the unmodified parent peptide. Further heteronuclear NMR experiments will be undertaken on a wide range of β-methylated analogs, which should provide complementary information on the rotameric populations for the side chain of the modified residues. In the present study, we focus our discussion on the change of conformational preferences of a particular side chain rotamer and the resulting change in binding potency. This allows us to refine our suggestion of particular side chain rotamers of the β-methylated residues important for receptor binding.

To further investigate the conformational effect of the di-β-methylation, we carried out 100-ps molecular dynamics simulations for the di-β-methylated analogs **III** and **IV**. The side chain conformations of β-MeTrp^8 and β-MePhe^{11} in the di-β-methylated analogs (**III**, **IV**) during dynamics simulations were compared with those of β-MeTrp^8 and β-MePhe^{11} in the mono-β-methylated analogs. Figure 5 shows the comparison of the

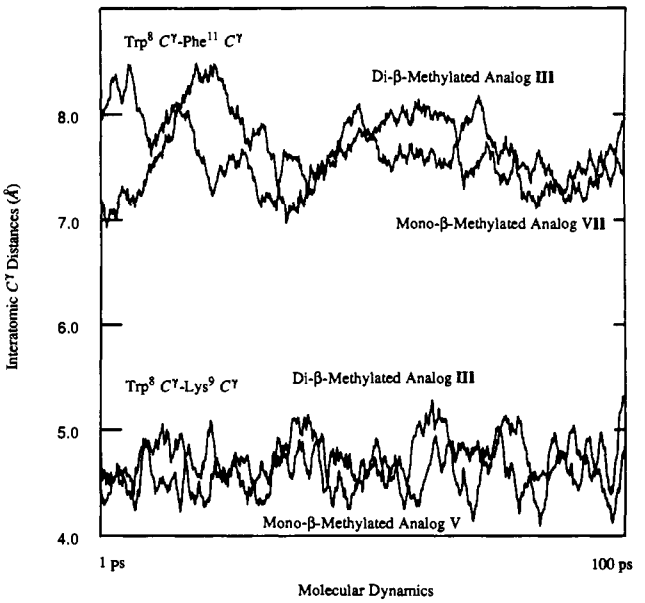

Figure 5. Interatomic distances during a 100-ps time course of molecular dynamics for the C^γ atoms of the Trp^8, Lys^9, and Phe^{11} side chains of the di-β-methylated analog **III** and mono-β-methylated analogs **V** and **VII**.

(25) Rose, G. D.; Gierash, L. M.; Smith, J. A. *Adv. Protein Chem.* **1985**, *37*.

(26) Arison, B. H.; Hirschmann, R.; Veber, D. F. *Bioorg. Chem.* **1978**, *7*, 447–451.

(27) NMR studies of c[-Pro^6-Phe^7-L-Trp^8-Lys^9-Thr^{10}-Phe^{11}-] indicated a β I turn around Trp^8-Lys^9. As for the bridging region, a *cis*/*trans* isomerism was observed for the amide bond between Phe^{11} and Pro^6 with a ratio of 83:17. The side chain of Phe^{11} at the bridging region displayed a predominant *trans* rotamer and essentially 0 population for the *gauche* rotamer: Huang, Z.; et al. Unpublished results of this laboratory.

side chain–side chain distances of β-MeTrp[8]-Lys[9] and β-MeTrp[8]-β-MePhe[11] during molecular dynamics for the bioactive di-β-methylated analog **III** and the mono-β-methylated analogs c[-Pro[6]-Phe[7]-(*2R,3S*)-β-MeTrp[8]-Lys[9]-Thr[10]-Phe[11]-] and c[Pro[6]-Phe[7]-D-Trp[8]-Lys[9]-Thr[10]-(*2S,3S*)-β-MePhe[11]-]. These side chain–side chain distances define the modified side chain topologies in the mono- and di-β-methylated analogs. As shown in Figure 5, the side chain topologies of β-MeTrp[8] and β-MePhe[11] in the di-β-methylated analog **III** are similar to those of β-MeTrp[8] and β-MePhe[11] in each of the corresponding mono-β-methylated analogs. These results, together with those from NMR studies, suggest that the constraining effect of the β-methylation at positions 8 and 11 in the monomethylated analogs is seen in the di-β-methylated analogs.

The binding potencies of the di-β-methylated analogs (**III, IV**) are also related to those of the mono-β-methylated analogs. As shown in Table I, the mono-β-methylated analog containing (*2R,3S*)-β-MeTrp[8] (**V**) shows higher potency than the parent compound (**I**), while the mono-β-methylated analog containing (*2S,3S*)-β-MePhe[11] (**VII**) shows a 50-fold decrease in binding potency. The dimethylated analog **III** containing both (*2R,3S*)-β-MeTrp[8] and (*2S,3S*)-β-MePhe[11] shows binding potency intermediate between the mono-β-methylated analogs **V** and **VII**. In addition, both the mono-β-methylated analog containing (*2S,3R*)-β-MeTrp[8] (**VI**) and the mono-β-methylated analog containing (*2S,3S*)-β-MePhe[11] (**VII**) show decreases in binding potency by 10- and 50-fold, respectively. The dimethylated analog **IV** containing both (*2S,3R*)-β-MeTrp[8] and (2*S*,3*S*)-β-MePhe[11] shows low potency, which may be explained by the combined effect from the mono-β-methylation at positions 8 and 11 in the corresponding mono-β-methylated analogs **VI** and **VII**.

Conclusions

We have investigated the bioactive conformation of somatostatin utilizing the approach of main chain and side chain methylations of a cyclic hexapeptide analog. An analog containing α-methylation at position 10 and two analogs containing β-methylations at both position 8 and 11 have been synthesized. The conformational and biological effects of main chain and side chain methylations in these somatostatin analogs have been analyzed by ^{1}H-NMR experiments and computer simulations. Conformational studies of the α-MeVal[10] analog indicated that this molecule displays a flat conformation and does not bind. On the basis of this study and our prior report on the α-MePhe[7] analog, we now contend that α-methylation at either residue 7 or 10 constrains the molecule to prefer the flat conformation, which leads to the loss of binding affinity. The studies of di-β-methylated analogs also provided insight on the side chain conformation of Trp[8] and Phe[11], important for receptor binding. The NMR experiments and molecular dynamics simulations indicated that the side chains of β-MeTrp[8] and β-MePhe[11] are constrained by β-methylations to prefer *trans* and g^- rotameric conformations, respectively. We can now conclude that di-β-methylated analogs display constrained side chain conformations for the β-methylated residues similar to those of mono-β-methylated analogs and retain appropriate binding potencies. The dimethylated analog **III** containing a β-methylated D-Trp[8] retains high binding potency. The dimethylated analog **IV** containing a β-methylated L-Trp[8] shows low binding potency, which may be explained by the combined loss of binding potency because of the β-methylation at both position 8 and 11. Conformational and biological studies of the di-β-methylated analogs suggest that the *trans* side chain conformation for both D-Trp[8] and Phe[11] residues is important for the receptor binding. This approach of using main chain and side chain methylations to derive the bioactive conformation of somatostatin analogs should have important implications in the study of other biologically active peptides.

Experimental Section

General Data. Melting points, determined on a Thomas-Hoover capillary melting point apparatus, were uncorrected. The optical rotations were measured on a Perkin-Elmer 141 polarimeter with a 10.001-cm thermostated cell. Nuclear magnetic resonance spectroscopy of the amino acid derivatives and dipeptides was carried out on a General Electric QE-300 spectrometer. Fast atom bombardment mass spectra were obtained from the University of California, Riverside. Amino acid analysis was performed at Scripps Research Institute, La Jolla, CA. High-pressure liquid chromatography was run on Waters HPLC systems, equipped with two 510 solvent pumps, a Waters 484 detector, and a Perkin-Elmer LC1-100 integrator (system 1) or equipped with two m45 solvent pumps, a Kratos Spectroflow 757 detector, and a Hewlett-Packard 3396 series II integrator (system 2). Thin-layer chromatography was carried on silica gel 60 (F_{254}) plates using the following solvent systems: (A) $CHCl_3$/MeOH/AcOH, 22:1:1; (B) $CHCl_3$/MeOH/NH_4OH, 85:32:5. The compounds were visualized by UV light, chlorine/*o*-tolidine, ninhydrin, and vanillin.

Boc-Lys(2Cl-Z)-(*S*)-α-MeVal-OMe. A methanol solution (50 mL) of the optically pure (*S*)-H-α-MeVal-OH (1.50 g, 11.45 mmol) and thionyl chloride (5 mL) was refluxed for 4 days. During the reaction, thionyl chloride (5 mL) was added each day. After removal of the solvent, the crude product, HCl-(*S*)-H-α-MeVal-OMe, was dissolved in DMF (100 mL), and the solution was cooled to −40 °C. The mixture was neutralized by DIEA, and then Boc-Lys(2Cl-Z)-OH (3.24 g, 7.81 mmol), BOP (5.12 g, 11.57 mmol), and DIEA (1.49 g, 11.57 mmol) were added. The reaction mixture was warmed to room temperature and stirred for 24 h followed by concentration under reduced pressure. The residue was diluted with ethyl acetate (200 mL), washed with an aqueous solution of $NaHCO_3$ and brine, dried over $MgSO_4$, and then concentrated. Column chromatography on silica gel (hexane/ethyl acetate 5:5) gave 3.95 g (64%) of Boc-Lys(2Cl-Z)-(*S*)-α-MeVal-OMe as a white solid: mp 45.0–46.5 °C; $[\alpha]^{25}_D$ −7.76°; ^{1}H-NMR (DMSO-d_6) δ 7.77 (s, 1H, CONH, α-MeVal), 7.48–7.30 (m, 5H, ClPh, CONᵋ-H), 6.72 (d, 1H, CONH, J = 8.1 Hz), 5.08 (s, 2H, 2Cl-Z), 3.98–3.87 (m, 1H, Cᵅ-H), 3.52 (s, 3H, OMe), 3.05–2.92 (m, 2H, Cᵋ-H), 2.01–1.90 (m, 1H, Cᵝ-H, α-MeVal), 1.61–1.20 (m, 6H, Cᵝ,ᵞ,ᵟ-H), 1.37 (s, 9H, Boc), 1.29 (s, 3H, α-Me), 0.91 (d, 3H, β-Me, J = 6.6 Hz), 0.81 (d, 3H, β-Me, J = 6.6 Hz); MS m/z 542 $(M+H)^+$; HR-MS calcd for $C_{26}H_{41}N_3O_7Cl$ $(M+H)^+$ m/z 542.2633, found 542.2628.

Boc-Lys(2Cl-Z)-(*S*)-α-MeVal-OH. A mixture of Boc-Lys(2Cl-Z)-(*S*)-α-MeVal-OMe (940 mg, 1.74 mmol) and LiOH (117 mg, 2.78 mmol) in H_2O (5 mL) and MeOH (14 mL) was stirred at room temperature for 1 day, and a second portion of LiOH (146 mg, 3.48 mmol) was added. The reaction mixture was stirred for 2 weeks, followed by concentration under reduced pressure at room temperature. The residue was acidified to pH 3.5–4 with an aqueous solution of sodium bisulfate, extracted with ethyl acetate (3 × 100 mL), dried over $MgSO_4$, and then concentrated. Column chromatography on silica gel (hexane/ethyl acetate 7:3, followed by chloroform/methanol 9:1) gave 738 mg (81%) of the product as a white solid: mp 49.0–50.0 °C; $[\alpha]^{25}_D$ −8.47°; R_f(A) 0.48; ^{1}H-NMR (DMSO-d_6) δ 12.40 (br, 1H, COOH), 7.83 (s, 1H, CONH, α-MeVal), 7.49–7.30 (m, 5H, ClPh, Nᵋ-H), 7.01 (d, 1H, CONH, J = 6.9 Hz), 5.07 (s, 2H, 2Cl-Z), 3.78–3.60 (m, 1H, Cᵅ-H), 3.01–2.90 (m, 2H, Cᵋ-H), 2.31–2.18 (m, 1H, Cᵝ-H, α-MeVal), 1.64–1.08 (m, 6H, Cᵝ,ᵞ,ᵟ-H), 1.37 (d, 3H, α-Me), 1.34 (s, 9H, Boc), 0.92 (d, 3H, β-Me, J = 6.6 Hz), 0.79 (d, 3H, β-Me, J = 6.6 Hz); MS m/z 492 $(M-Cl)^+$, 428$(M-Boc+H)^+$.

Synthesis of Cyclic Hexapeptide c[-Pro-Phe-D-Trp-Lys-(*S*)-α-MeVal-Phe-] (II).[28] The peptide synthesis was carried out on a manually operated solid-phase synthesis apparatus. Boc-Trp(For)-OH (585 mg, 1.76 mmol) was attached to oxime resin[29] (4.50 g) with DCC (362 mg, 1.76 mmol) in DCM (70 mL) at room temperature overnight, followed by acylation with a mixture of pivalic anhydride (6.75 mL) and DIEA (2.25 mL) in DCM (60 mL) for 3 h, yielding 4.70 g (substitution level 0.28 mmol/g of resin based on picric acid titration,[30] 1.32 mmol of amino acid). The obtained Boc-Trp(For)-resin was deprotected with 25% TFA/DCM (30 min) and neutralized with 5% DIEA/DCM. A DMF solution of Boc-Phe-OH (1.75 g, 6.60 mmol), BOP (2.92 g, 6.60 mmol), and DIEA (681 mg, 5.27 mmol) was poured into the reaction vessel. The coupling reaction was complete in 6 h. The peptide chain elongation was continued by consecutive deprotection of Boc groups and addition of the following amino acids and dipeptide: Boc-Pro-OH, Boc-Phe-OH, and Boc-Lys-

(28) All the washing steps were omitted.
(29) DeGrado, W. F.; Kaiser, E. T. *J. Org. Chem.* **1980**, *45*, 1295–1300.
(30) Gisin, B. F. *Anal. Chim. Acta* **1972**, *58*, 248–249.

(2Cl-Z)-(S)-α-MeVal-OH. The product, Boc-Lys(2Cl-Z)-α-MeVal-Phe-Pro-Phe-D-Trp(For)-resin, was obtained. After the Boc group was cleaved, the cyclization reaction was carried out on the resin in DCM (45 mL) and DMF (45 mL) in the presence of 10 equiv of AcOH at room temperature for 48 h. The crude cyclic peptide was obtained after filtration and evaporation: R_f(A) 0.45; FABMS m/z 1038 $(M + Na + H)^+$. The peptide was treated with HF/anisole/skatole (20 mL/2.5 mL/5 mg) at −10 °C for 30 min and at 0 °C for 30 min to give an oily material, which was treated with piperidine (25 mL) for 3 h at room temperature. Purification of the final product was carried out on RP-HPLC (system 2; Vydac C_{18} proteins semipreparative column; gradient from 30 to 42% CH_3CN/H_2O with 0.1% TFA over 30 min; flow rate 4 mL/min; detection at 215 nm) to give 13 mg of c[-Pro-Phe-D-Trp-Lys-α-MeVal-Phe-] (II) (1% based on the starting Boc-D-Trp(For)-resin): R_f(B) 0.68; t_R 14.1 min (system 2, Vydac C_{18} proteins semipreparative column; eluent 37% CH_3CN/H_2O with 0.1% TFA; flow rate 4 mL/min; detection at 215 nm); amino acid analysis Lys 1.00, Phe 2.22, Pro 0.89, Trp 0.80; MS m/z 819 $(M + H)^+$, 841$(M + Na)^+$, 857$(M + K)^+$; HR-MS calcd for $C_{46}H_{59}N_8O_6$ $(M + H)^+$ m/z 819.4557, found 819.4561.

Syntheses of Cyclic Hexapeptides: c[-Pro-Phe-(2*R*,3*S*)-β-MeTrp-Lys-Thr-(2*S*,3*S*)-β-MePhe-] (III) and c[-Pro-Phe-(2*S*,3*R*)-β-MeTrp-Lys-Thr-(2*S*,3*S*)-β-MePhe-] (IV).[28] The peptide synthesis was carried out on a manually operated solid-phase synthesis apparatus. Boc-Thr(OBzl)-Merrifield resin (700 mg, substitution level 0.73 mmol/g of resin, 0.511 mmol of amino acid) purchased from BACHEM was deprotected with TFA/anisole/DCM (50:2:48) (30 min) and neutralized with 5% DIEA/DCM. A DMF solution of Boc-Lys(Fmoc)-OH (693 mg, 1.53 mmol), BOP (678 mg, 1.53 mmol), and DIEA (263 mg, 2.04 mmol) was poured into the reaction mixture. The coupling reaction was complete in 2 h, indicated by the Kaiser test. The peptide chain was then assembled by consecutive deprotection of Boc groups and addition of Boc-(2*R*,3*S* + 2*S*,3*R*)-β-MeTrp-OH, Boc-Phe-OH, Boc-Pro-OH, and Boc-(2*S*,3*S*)-β-MePhe-OH as above. Thus, Boc-(2*S*,3*S*)-β-MePhe-Pro-Phe-(2*R*,3*S* + 2*S*,3*R*)-β-MeTrp-Lys(Fmoc)-Thr(OBzl)-resin was obtained. Amino acid analysis: Lys 1.00, Thr 1.01, Phe 1.08, Pro 1.04. The above peptidyl resin was treated with HF/anisole/skatole (20 mL/1.2 mL/10 mg) at −10 °C for 30 min and at 0 °C for 30 min. The resulting peptide was dissolved in AcOH (80%, 15 mL), and the resin was removed by filtration. Separation and purification of the two diastereomers were carried out on RP-HPLC (system 1; Waters C_4 proteins preparative cartridge; eluent 46% CH_3CN/H_2O with 0.1% TFA; flow rate 7 mL/min; detection at 215 nm). H-(2*S*,3*S*)-β-MePhe-Pro-Phe-(2*R*,3*S*)-β-MeTrp-Lys-(Fmoc)-Thr-OH: yield 128 mg (42% based on the starting Boc-Thr-(OBzl)-resin); t_R 41.2 min; R_f(B) 0.61; amino acid analysis Lys 1.00, Thr 1.15, Phe 1.12, Pro 1.13; FABMS m/z 1076 $(M + 2H)^+$. H-(2*S*,3*S*)-β-MePhe-Pro-Phe-(2*S*,3*R*)-β-MeTrp-Lys(Fmoc)-Thr-OH: yield 150 mg (49% based on the starting Boc-Thr(OBzl)-resin); t_R 26.1 min; R_f(B) 0.57; amino acid analysis Lys 1.00, Thr 1.08, Phe 1.08, Pro 1.09; FABMS m/z 1075 $(M + H)^+$.

The compound H-Phe-Pro-Phe-(2*R*,3*S*)-β-MeTrp-Lys(Fmoc)-Thr-OH (90 mg, 0.075 mmol) was dissolved in DMF (74 mL). DPPA (31 mg, 0.113 mmol), DMF (1 mL), and K_2HPO_4 (71 mg, 0.408 mmol) were added under nitrogen at 0 °C. The coupling reaction was carried out at 4 °C for 5 days, Bio-Red (AG 501-X8(D)) (2.0 g) was then added, and the mixture continued to stir at 4 °C for 2.5 h. After filtration, the solution was evaporated under reduced pressure, and the residue was treated with piperidine (15 mL) for 4 h at room temperature. Purification of the final product c[-Pro-Phe-(2*R*,3*S*)-β-MeTrp-Lys-Thr-(2*S*,3*S*)-β-MePhe-] (III) was carried out on RP-HPLC (system 1; Vydac C_{18} proteins preparative column; eluent 38% CH_3CN/H_2O with 0.1% TFA; flow rate 8 mL/min; detection at 215 nm): yield 16.5 mg (10% based on Boc-Thr(OBzl)-resin); t_R 33.3 min; R_f(B) 0.50; amino acid analysis Lys 1.00, Thr 1.02, Phe 1.05, Pro 0.93; FABMS m/z 835 $(M + H)^+$, 857 $(M + Na)^+$; HR-FABMS calcd for $C_{46}H_{59}N_8O_7$ $(M + H)^+$ m/z 835.4507, found 835.4523. c[-Pro-Phe-(2*S*,3*R*)-β-MeTrp-Lys-Thr-(2*S*,3*S*)-β-MePhe-] (IV) was obtained by the same cyclization method from H-(2*S*,3*S*)-β-MePhe-Pro-Phe-(2*S*,3*R*)-β-MeTrp-Lys(Fmoc)-Thr-OH: yield 15.0 mg (10% based on Boc-Thr(OBzl)-resin); t_R 29.4 min; R_f(B) 0.50; amino acid analysis Lys 1.00, Thr 0.88, Phe 1.01, Pro 1.15; FABMS m/z 835 $(M + H)^+$, 857 $(M + Na)^+$; HR-FABMS calcd for $C_{46}H_{59}N_8O_7$ $(M + H)^+$ m/z 835.4507, found 835.4543.

Binding Procedures. The binding of different peptides to the somatostatin receptor was performed as previously described.[31] Briefly, AtT-20 cells, which express a high density of somatostatin receptor, were detached from the culture flasks in which they were growing in phosphate-buffered saline, the cells were homogenized with a Brinkman Polytron (setting 1, 15 s), and the membranes were centrifuged at 20000*g* for 15 min at 4 °C. The pellet was resuspended, and the membranes were incubated in a buffer containing 50 mM Tris-HCl (pH 7.4), 1 mM EDTA, 5 mM $MgCl_2$, 10 ug/mL leupeptin, 10 ug/mL pepstatin, 200 ug/mL bacitracin, and 0.5 ug/mL aprotinin with 0.05 nM ^{125}I-MK 678 (specific activity 2000 Ci/mmol) in the presence or absence of various somatostatin analogs for 60 min at 25 °C. The reaction was terminated by adding 15 mL of ice-cold Tris-HCl (pH 7.8) buffer and vacuum filtering under reduced pressure over Whatman GF/C glass fiber filters. Radioactivity was assessed in a gamma counter (80% efficiency). Nonspecific binding was determined by the residual radioligand binding remaining in the presence of 1 μM somatostatin, and specific binding accounted for 80–85% of total ^{125}I-MK 678 binding. The potency of each peptide for the somatostatin receptor was assessed by determining the ability of different concentrations of the peptide to inhibit ^{125}I-MK 678 binding and then analyzing the inhibition curve using the PROPHET data analysis system. Affinities are expressed as IC_{50} values, and each IC_{50} is the averaged results of three different experiments for each peptide.

NMR Measurements. The ^{1}H-NMR spectra were recorded on either a General Electric GN-500 or a Bruker AMX spectrometer operating at 500 MHz. Temperatures were maintained at given values within ±0.1 °C during measurements. The samples were prepared in DMSO-d_6 purchased from Merck Sharp and Dohme Canada Ltd. at a concentration of 5–15 mM. DMSO-d_6 (=2.49 ppm) was used as an internal standard.

The one-dimensional spectra contain 16K data points in 6000–7000 Hz. The two-dimensional homonuclear Hartmann–Hahn (HOHAHA) experiments[32] were carried out using MLEV17[33] and the time proportional phase increment.[34] A mixing time of 100 ms (48 cycles of MLEV sequence) with a spin locking field of 10.2 kHz was employed. The rotating frame nuclear Overhauser (ROESY) experiments[35] were carried out varying the mixing time from 75 to 500 ms with a spin locking field of 2.5 kHz. All of the two-dimensional spectra were obtained using 2K data points in the f_2 domain and 256 points in the f_1 domain. Applying the zero-filling procedure to the f_1 domain twice resulted in a final matrix of 2K × 2K data points. Multiplication with either a phase-shifted sine or Gaussian function was used to enhance the spectra.

Computer Simulations. All calculations were performed on a Personal Iris 4D-25 workstation and an Iris 4D-340 computer (Silicon Graphics). Energy minimizations and molecular dynamics were carried out with the molecular modeling package which included QUANTA 3.0 (Molecular Biosystems Inc.) and CHARMM.[36]

All hydrogen atoms were included in all calculations. The potential energy of the molecular system was expressed by the valence force field implemented in CHARMM (without an explicit hydrogen-bonding term) with the PARM21A parameter set. A neutral form of the amine group in the Lys side chain was used. To approximate the solvation, all calculations were carried out at a distance-dependent dielectric constant ($\epsilon = R$)[37] unless specified otherwise. Energy minimizations with respect to all the Cartesian coordinates were carried out using the adopted basis Newton–Raphson (ABNR) algorithm[36] until all derivatives were smaller than 0.001 kcal/mol Å.

Molecular dynamics simulations were undertaken by numerical integration of Newton's equations of motion with a second-order predictor two-step Verlet algorithm.[38] The SHAKE algorithm[39] was used, which allowed a step size of 1 fs in dynamics. All simulations were preceded by 1 ps of heating from 0 to 300 K, followed by a 2-ps equilibration period. Equilibrations and simulations were performed at 300 K. NOE constraints were not used in dynamics calculations.

Acknowledgment. We wish to thank the National Institutes of Health (DK 15410) for their support of this research.

(31) Raynor, K.; Reisine, T. *J. Pharmacol. Exp. Ther.* **1989**, *251*, 510–517.
(32) Davis, D.; Bax, A. *J. Am. Chem. Soc.* **1985**, *107*, 2820–2821.
(33) Bax, A.; Davis, D. G. *J. Magn. Reson.* **1985**, *65*, 355–360.
(34) Bodenhausen, G.; Vold, R. L.; Vold, R. R. *J. Magn. Reson.* **1980**, *37*, 93–106.
(35) Bothner-By, A. A.; Stephens, R. L.; Lee, J.; Warren, C. D.; Jeanloz, R. W. *J. Am. Chem. Soc.* **1984**, *106*, 811–813.
(36) Brooks, B. R.; Bruccoleri, R. E.; Olafson, B. D.; States, D. J.; Swaminathan, S.; Karplus, M. *J. Comput. Chem.* **1983**, *4*, 187–217.
(37) McCammon, J. A.; Wolynes, P. G.; Karplus, M. *Biochemistry* **1979**, *18*, 927–942.
(38) Verlet, L. *Phys. Rev.* **1967**, *159*, 98–103.
(39) Van Gunsteren, W. F.; Berendsen, H. J. C. *Mol. Phys.* **1977**, *34*, 1311.